Research Article Vol. 13, No. 9 / 1 Sep 2023 / Optical Materials Express 2595
Optical Materials EXPRESS

Observation of amplified spontaneous emission in $Cd_{1-x}Zn_xSe$/ZnSe alloyed quantum dots through CW pumping

PALASH KUSUM DAS,[1] NISHANT DHIMAN,[2] SIVA UMAPATHY,[1,2] AND ASHA BHARDWAJ[1,*]

[1]Instrumentation and Applied Physics, Indian Institute of Science, Bengaluru, 560012, India
[2]Inorganic and Physical Chemistry, Indian Institute of Science, Bengaluru, 560012, India
[*]asha@iisc.ac.in

Abstract: Colloidal quantum dots (QDs) have attracted much attention due to their optical tunability and application as a unique solution processable gain medium in lasers. Many research groups over the world have successfully attained amplification from Cd-based QDs through femtosecond (fs) and nanosecond (ns) pumping. However, for the wide application of QD-based lasers, an operation in the CW regime is much more favorable. Here, we present a critical step towards this goal by demonstrating CW laser (532 nm) pumped amplified spontaneous emission (ASE) in $Cd_{1-x}Zn_xSe$/ZnSe alloyed core QDs dispersed in toluene at room temperature. Alloyed core QDs show lower non radiative transitions, which has been demonstrated by TA dynamics in this report. The threshold level for CW ASE is observed to be 31 W cm^{-2}. These results indicate that these QDs can sustain CW-stimulated emission at room temperature, and can be widely applicable by further optimizing the QD material quality in order to have a low amplification threshold.

1. Introduction

In the frame of developing novel active materials for electronic, optoelectronic and photonic devices, Cd based quantum dots (CQDs) are currently receiving great attention due to their capability to combine an easy realization procedure, widely tunable optical properties and promising performance as active materials for wide range of applications [1]. The capacity to defeat opposing non-radiative mechanisms forms the cornerstone for achieving optical gain in quantum dots.

CQD preparations in solution or solid thin film has led to a number of gain models based on multi-exciton states (per CQD). In multi-exciton systems, inelastic electronic interactions invariably result in strong intrinsic non-radiative Auger recombinations. It appears beyond doubt that the many-body Auger events can result in significant inhibition and depletion of multi-excitonic gain on a sub-nanosecond time frame because of the severe spatial confinement. In particular, CdSe/CdS QDs have an impressive advancement in achieving solution processable QD based lasing. Numerous research teams concentrated on boosting absorption cross-sections utilising large-volume nanostructures such as nanorods [2,3], giant-shell QDs [4], tetrapods [5], nanoplatelets [6,7], large-sized perovskite nanocrystals and nanowires [8,9,9,10] in order to achieve low gain threshold. The Auger recombination issue has been addressed in a number of parallel efforts by adjusting the QD volume factor [4] and the confinement potential shape [11] or by utilising cutting-edge lasing concepts like "single-exciton gain," which is realised through strong exciton-exciton repulsion [12]. Through photodoping, Victor et al. showed zero threshold lasing [13]. There is also report on use of distributed feedback (DFB) lasers [14,15], optically pumped vertical cavity surface emitting lasers (VCSEL) [16], and photonic crystal coherent emitters [17,18] in CQD laser demonstrations. II-VI colloidal nanocrystalline platelets

#495483 https://doi.org/10.1364/OME.495483
Journal © 2023 Received 23 May 2023; revised 17 Jul 2023; accepted 18 Jul 2023; published 21 Aug 2023

Optical Materials EXPRESS

are a recent addition to the field, and very recent work on ASE and lasing have been reported at incredibly low optical excitation levels [19,20].

However, despite considerable progress over the past decade, QD lasing is still not a commercial technology. Any novel gain material must, however, show the ability to maintain optical gain under continuous wave (CW) operation and ideally at RT, or at least at temperatures reachable by Peltier cooling (>220 K), in order to become widely applicable (ultimately in an electrically pumped configuration) [21]. Earlier, [22] showed ASE with HgTe QDs by intentional trap states that paves the way for solution-processed infrared QD lasers and amplifiers. Recent research on perovskite nanocrystals used for ASE has also been published. Examples include enhanced amplified spontaneous emission from ultrastable $CsPbBr_3$ perovskite quantum dots by surface ligand modification [23]; improved photoresponse of a self-powered perovskite photodetector using ZnO nanoparticles ornamented $CsPbBr_3$ films [24]. Modified $CsPbBr_3$ perovskite quantum dots exhibit stable and low-threshold whispering-gallery-mode lasing [25]; stable $CsPbBr_3$ quantum dots exhibiting amplified spontaneous emission are synthesised at room temperature by [26]. Wang et al. demonstrated ultra-low threshold of 15 W cm^{-2} with CW excitation at room temperature with DFB configuration [27]. Li Jiang et, al. obtained nano laser from perovskite nanowire with CW pumping at 4 K temperature [28]. H. Zhang et, al. demonstrated lasing from vertical cavity surface-emitters based on single lead halide perovskites at 80 K [29]. His group also developed lasing from organic–inorganic hybrid perovskites operating at RT with CW excitation [30]. MS Alias et, al. reported optically pumped green perovskite vertical-cavity surface-emitter operating in continuous-wave (CW) with a power density threshold of ~ 89 kW cm^{-2} [31]. Qin et, al. reported CW-pumped lasing in perovskite thin film with threshold of 45 W cm^{-2} [32]. In this sense, although the previous reports show incredible achievements, obtaining ASE with CW pump, suppressing auger recombination is a major challenge.

Alloying QDs, on the other hand, can greatly minimize auger recombination in QDs because it provides better control over the energy levels of the carriers. By altering the QD's composition, the bandgap can be designed to match the energy levels of the carriers, lowering the energy required for recombination and reducing the likelihood of auger recombination. Furthermore, alloyed QDs have soft confinement of electrons and holes, and more uniform distribution of strain within the QDs, thus leading to suppression of non-radiative recombination pathways and improving the efficiency of the QD-based devices [33–37]. In $Cd_{1-x}Zn_xSe/ZnSe$ alloyed core-shell QDs, auger recombination is reduced by one order of magnitude from typical CdSe QDs leading to increased multi-exciton lifespans [38,39]. This material with quantum well structure has already demonstrated potential in lasing with pulse current injection [39,40].

Keeping in mind the fascinating properties of $Cd_{1-x}Zn_xSe/ZnSe$ alloyed core-shell QDs conducive for optical gain, in this work a further optimization of the material was carried out in order to observe gain using CW laser at RT. The QDs were first optimised for their emission and absorption characteristics and then further used for observing gain. Emission maxima of the QDs was attained at 654 nm with a Quantum Yield (QY) of 58%. Further, optical gain in QDs in the cuvette is attained by using a fs-pulsed laser (average power 1 μW cm^{-2}) using transient absorption (TA) spectroscopy. A CW- laser (532 nm) and an external source with 654 nm wavelength (similar to QD emission) have been utilized in the same configuration to produce amplified spontaneous emission (ASE). Compared to the other groups [23–32], in this report 31 W cm^{-2} CW pumped ASE at RT has been demonstrated. Thus, such ASE at RT with QDs dispersed in toluene, after further extensive development, could be a good candidate for realizing solution-processable QD lasers in the future.

Optical Materials EXPRESS

2. Experimental section

2.1. Synthesis of QDs

The "hot injection" method was used to generate high-quality Zn-rich $Cd_{1-x}Zn_xSe/ZnSe$ core/shell QDs with a slight modification from [41]. In our synthesis, 0.1 mmol of CdO and 1 mmol of ZnO were combined with 8.85 mmol of oleic acid and 15 ml of octadecene (ODE) and degassed for 2 minutes in a 3-neck flask. Later, in an inert atmosphere, the flask was heated to 300 °C. At this temperature, a Se precursor was quickly injected by dissolving 0.08 mmol of Se in 0.2 ml of TOP and 2 ml of ODE. Further, the QDs were washed and dispersed in chloroform. When exposed to UV light, QDs emit a strong red light (Fig. 1(f) inset).

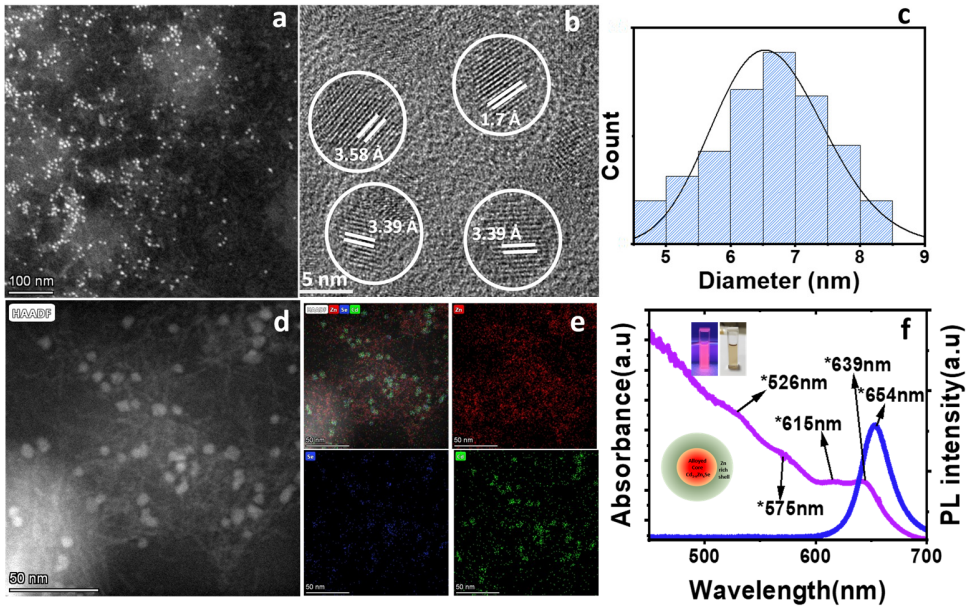

Fig. 1. **a** STEM image of $Cd_{1-x}Zn_xSe/ZnSe$ QDs (lower magnification), **b** HRTEM image shows crystalline nature and spherical shape of the Quantum dots. The lattice spacings estimated from the image correspond to bulk ZnSe crystal **c** shows the size distribution histogram of the QDs, which have a mean at 6.5 nm **d** HDAAF-STEM image of QDs **e** shows the corresponding composition elemental mapping. It shows that the QDs formed are rich in Zinc. Similar results were also found in EDS spectra taken at a particular QD which also corroborated higher Zinc percentage (67%) **f** absorption and photoluminescence spectrum of the QDs with upper inset showing QD under UV light and daylight & lower inset shows schematic of the as fabricated QDs.

2.2. Transient absorption spectroscopy (TA)

A Ti: sapphire regenerative amplifier (Spitfire, Spectra Physics) with an output of roughly 2 mJ/pulse and a pulse width of 100 fs centred at 790 nm was used to amplify 100 fs seed pulses produced by a Ti: sapphire oscillator (Tsumani, Spectra Physics) at a repetition rate of 1 kHz. The increased 1 mJ/energy pulses were divided into two equal portions (95:5) using a beam splitter. TOPAS-C (Spectra-Physics) was pumped with 95% of the available energy to construct a 370 nm actinic pump. The remaining 5% of the light is focused on a 3 mm CaF_2 crystal to form a broadband super-continuum white light (380-720 nm) probe. The pump and probe beams were kept at Magic-angle (54.70°). To avoid photodegradation of the sample, both beams were spatially overlapped on the moving 1 mm sample cuvette. To enter the spectrograph (Triax 550,

Optical Materials EXPRESS

Horiba), a transmitted white light probe and reference beam were chosen and dispersed by a 150 mm grooves/mm grating.

2.3. Experimental setup for obtaining ASE in the cuvette

A cuvette containing 1.5×10^{-5} mmol of the $Cd_{1-x}Zn_xSe$/ZnSe QDs dissolved in 3 ml of toluene was used to observe ASE. The sample was pumped with a 532 nm CW laser source. Additionally, as shown in Fig. 3(a), a monochromator-based lamp was fed into the sample at a normal incidence, generating light at 654 nm (FWHM = 18 nm), the same wavelength as the maximum PL of the QDs. A 20x microscopic objective lens was used to collect the final emission at 90° angle to the laser beam, and the emission was recorded in an Optical Spectrum Analyzer.

2.4. Characterization

For structural characterization, TEM and High Resolution-TEM has been done. To understand the composition, EDS has been done. For optical characterization, photoluminescence (PL) and absorption have been taken.

3. Result & discussion

The STEM image (Fig. 1(a)) demonstrates the spherical morphology of the QDs. The QDs have an average size of 6.5 ± 1 nm (diameter), which is being depicted by a histogram in Fig. 1(b). Lattice spacing was determined to be 1.70 Å (300), 3.58 Å (100), and 3.39 Å (111), from HRTEM image (Fig. 1(b)), which corresponds to the ZnSe cubic structure. EDS corroborated the highest percentage of Zn, 67%, as compared to 19% Cd and 16% Se, which indicates that these QDs are rich in Zn and have more than one ZnSe shell covering their outer layer (Figure S1). The STEM-HDAAF image also shows the three-dimensional spherical nature of the QDs (Fig. 1(d)) and STEM elemental mapping (Fig. 1(e)) demonstrates that the zinc content of the as synthesized QDs is more compared to Cd and Se. The schematic $Cd_{1-x}Zn_xSe$/ZnSe core-multi-shell structure is shown in Fig. 1(f) (inset), which has been drawn by following the above structural analysis.

The QDs have an emission peak at 654 nm with FWHM of ~ 34.5 nm, and absorption peaks at 639 nm, 615 nm, 575 nm, and 526 nm (Fig. 1(f)). Figure S2 and S3 shows the absorbance and PL properties of the QDs with growth time. Figure S4 shows the PL peak shift and FWHM with growth time of the QDs.

Further, potential of these QDs for optical gain was evaluated using ultrafast transient absorption (TA) spectroscopy to measure the temporal nonlinear optical characteristics of QDs dispersed in toluene. Gain properties of the QDs has been analyzed through fs pumping (100 fs) before examining them under CW pumping.

Here, the QDs are pumped with ultra-short laser pulses using the pump-probe method, and the change in absorbance ΔA is then measured as a function of wavelength by a time-delayed probe pulse. ΔA is expressed as:

$$\Delta A = A_{ex} - A_0 \tag{1}$$

Where A_{ex} = absorption spectrum when the sample is in an excited state and A_0 = steady state absorption. In the TA spectrum, ΔA is obtained after exciting the sample with 370 nm pulsed laser (Fig. 2(a)). The TA spectrum shows three bleaching spots, which are located at 639 nm, 615, 575 nm and 525 nm. The first three spots are attributed to the QD transitions 1S(e)-$1S_{3/2}$(h), 1S(e)-$2S_{3/2}$(h) and 1P(e)-$1P_{3/2}$(h), respectively, while the final spot is caused by the transition in ZnSe shell.

To further understand the QD's gain characteristics, a separate A_0 is taken without altering the solution concentration, which ensures that the same absorption cross-section is maintained. A_{ex} is produced after the addition of A_0 with ΔA. A negative A_{ex} would mean a signal with a wavelength similar to the ground state transition (639 nm) has overpowered absorption in the

Optical Materials EXPRESS

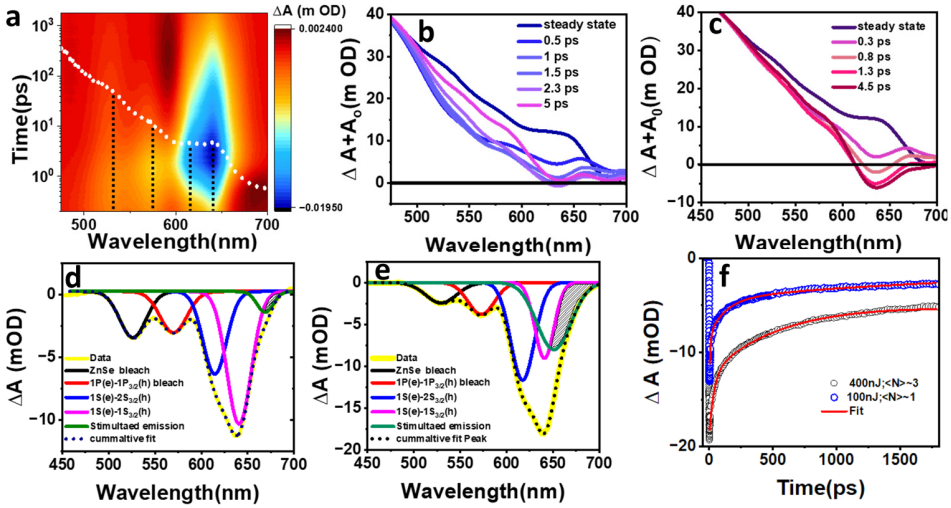

Fig. 2. **a** Transient Absorption spectrum after pumping at 370 nm, so that it excites both core (absorbs at 639 nm) and shell (absorbs at 525 nm) of QDs. It shows that ground state bleaching has a longer lifetime compared to bleaching at shell (the colour bar in the picture is in OD) **b** $\Delta A + A_o$ corresponding to $< N > \sim 1$ becoming 0 with an increase in time showing stimulated emission building up **c** $\Delta A + A_o$ corresponding to $< N > \sim 3$ showing efficient gain **d** Deconvoluted TA spectrum at 2.3 ps corresponding to $< N > \sim 1$, showing much higher strength of absorption than stimulated emission **e** Deconvoluted TA spectrum at 2.3 ps corresponding to $< N > \sim 3$, showing comparable strength of absorption and stimulated emission. **f** TA bleaching kinetics of ground state transition fitted with tri exponential curve.

system. In this way, it is possible to say that optical gain has been accomplished, meaning that if a signal of the same wavelength and phase is delivered, an enhanced signal will be picked up from the system. TA spectrum of the sample has been obtained at two different pump powers where one is much lower (100 nJ) so that exciton generation per QD, $<N> \sim 1$ and another one is much higher $< N > \sim 3$ per QD. A single exciton ($<N> = 1$) is produced when a valence band electron is excited to the conduction band. This condition is known as "QD optical transparency" because the valence band electron's absorption precisely balances the stimulated emission of the conduction band electron. Since the QDs are doubly degenerate, the second electron must be excited to the conduction band in order to obtain optical gain. In this case, the QD begins to enhance light after the absorption and complete state filling of the ground state. Therefore, optical gain is observed in the QDs when two electron-hole (e-h) pairs, also known as "biexcitons" are formed. This further implies that the gain threshold is reached when the average per-dot excitonic occupancy, $< N >$, approaches 1 and that the QD system becomes "inverted" when N exceeds 1. Following the addition of various ΔA at different time constants with steady-state absorption, nonlinear optical density has been obtained. From Fig. 2(b) it can be seen that $A_{ex} = \Delta A + A_o$ for $< N > \sim 1$, becomes zero after 2.3 picoseconds (ps) of excitation at 639 nm, demonstrating that gain precisely compensates for absorption. Whereas for $< N > \sim 3$, (Fig. 2(c)) A_{ex} becomes negative after 0.8 ps, which shows that an effective optical gain regime is achieved. With sufficient pump powers, appropriate exciton generation can overcome intrinsic non-radiative absorption and show amplification.

The TA spectrum is mainly composed of ground-state bleaching or excitation from the ground state to 1^{st} excitation state or transition $1S(e) - 1S_{3/2}(h)$ (optical absorption) and stimulated emission (optical gain). As a result, the TA spectrum has been deconvoluted in order to comprehend the competition between optical gain and optical absorption at a fixed delay time of

Optical Materials EXPRESS

t = 2.3 ps. According to the TA spectrum, the deconvoluted curve corresponding to < N > ~1 (Fig. 2(d)), ground state bleaching is much more intense than stimulated emission, whereas stimulated emission is significantly more intense for < N > ~3 (Fig. 2(e)). The intensity of the ground-state bleaching, however, remains constant in both cases. As a result of stimulated emission's ability to overcome ground state absorption, an overall enhanced signal is obtained at higher pump power.

A comparison of 1S exciton bleach recovery kinetics for pump power corresponding to < N > ~1 and < N > ~3 at 639 nm also has been done (Fig. 2(f)). The negative exponential recoveries were fitted with a summation of three exponential curves. The fitted values are given in Table 1. The fastest lifetime (τ_1) is attributed to interfacial or surface defect states, the moderate one (τ_2) is attributed to Auger recombination, and the slowest one ($\tau_3 > 1$ ns) is attributed to radiative recombination. In this instance, auger recombination rate serves as a direct indicator of biexciton lifetime. Gain lifetime is constrained by auger lifetime. The longer the auger lifespan, the longer the gain lifetime. It is evident that when pump power increases, the percentage of auger recombination also increases. This is due to the fact that more exciton production occurs as pump power increases.

Table 1. Fitted values of TA kinetics at 639 nm

	<N> ~1	<N> ~3
τ_1 (ps)	14	37
τ_2 (ps)	615	587
τ_3 (ps)	3374	3548
A_0(Offset)	-0.00651	-0.00647
A_1	-0.00686(37.6%)	-0.00664(38%)
A_2	-0.00677(33.5%)	-0.00834(47.7%)
A_3	-0.00658(32.5%)	-0.00251(14.4%)

To understand the light amplification property of the QDs through CW pumping, a cuvette (same as used for fs pumping) containing QDs were taken. Here, to the cuvette an external light signal having wavelength similar to PL peak (654 nm) of the QDs has been used and were fed to the QDs (Fig. 3(a)). This has been done to understand the amplification property of the QDs for some external signal (lamp). The emission signal has been taken in the presence of the lamp signal (QLS) by varying pump power of the QDs (QS). The power of the lamp signal is kept in such a manner so that it matches with the emission signal power excited with minimum pump power (10 mW) so that, if there is no amplification with pump power the difference between QS and QLS will always be same. The spot size of the pump is kept to be 1 mm. Figure 3(b) shows the emission profile of the system with and without the lamp by varying the pump power. Figure 3(c) shows that the QS intensity increases linearly regardless of the presence of the lamp. However, the slope (change in intensity/pump power) has a higher value for the QLS signal. Higher slope for QLS is because, as pump power increases, more QDs become excited. As a result, the lamp, which serves as feedback, can interact with more excited QDs, increasing the slope's value for the QLS signal. The overall enhancement in the signal with the help of the lamp has been calculated by simply subtracting the QS signal from the QLS signal (Fig. 3(c)). This enhancement is also called Amplified Spontaneous Emission (ASE). Clearly the amplification threshold can be seen to be at 150 mW (~19.1 Wcm^{-2}).

The sharp ASE that has been reported earlier has been obtained through sophisticated DBR which reflects specific wavelengths [14,15]. Here in this experiment, the lamp signal which has been used has an inbuilt FWHM of 18 nm along with QD size distribution, making the ASE emission broad. The main cause for observing ASE in such a configuration is because of the

Optical Materials EXPRESS

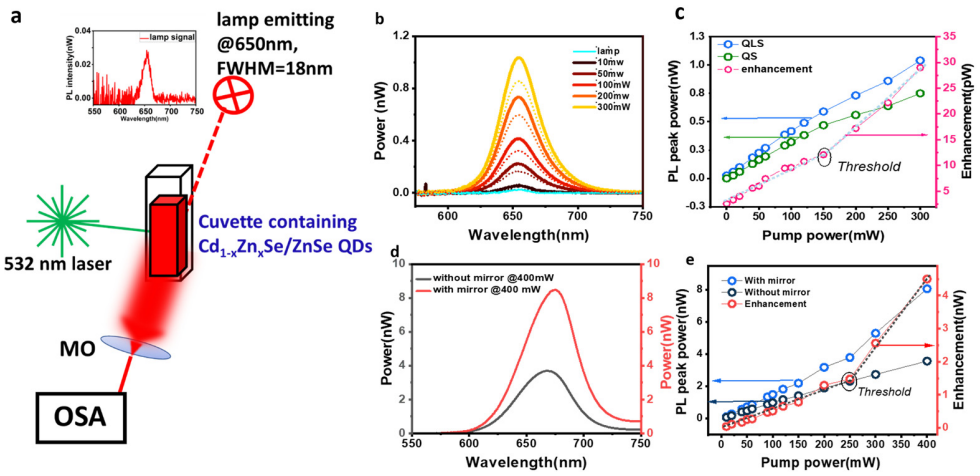

Fig. 3. **a** Schematic of the experimental setup to capture amplified spontaneous emission. **b** emission spectra without using lamp shown as dashed line and with using probe shown as solid lines by varying the input pump power **c** the peak power of emission with (blue) and without (green) using the external lamp at left y-axis along with the enhancement in the emission (pink) at right y-axis. **d** emission spectra with and without mirror when pump power is 400 mW. **e** the peak power of emission with (blue) and without (dark blue) using the mirror at left y-axis along with the enhancement in the emission (red) at right y-axis

feedback provided by the lamp to the QDs in the cuvette [42,43], which results in stimulated emission from the QDs. The enhancement observed is 1 order less than the emission signal because of the very low probability of phase matching of QDs with the lamp wavelength. In order to further increase the feedback, the lamp signal has been replaced with a mirror. The emission spectrum of the QDs with and without the presence of a mirror pumped at 400 mW is shown in Fig. 3(d). The PL peak power of the emission with and without mirrors and their difference in power is shown in Fig. 3(e). It is clearly evident that the signal taken in the presence of a mirror is higher compared to the signal taken without a mirror. The enhancement has a sharp threshold at 250 mW ($\sim 31.8\ \mathrm{Wcm^{-2}}$). The mirror as feedback, clearly demonstrates lasing cavity-like effect. Despite the greater threshold discovered with mirror feedback, the order of enhancement was higher (in nW) when compared to enhancement with an external lamp (in pW). Since these QDs are toluene-dispersed, the heat generated by the pump is easily distributed in the solution, and the large volume of toluene acts as a heat sink, which stabilizes the system.

4. Conclusion

In conclusion, structural characteristics of $Cd_{1-x}Zn_xSe/ZnSe$ QDs were investigated through a TEM, HRTEM and STEM and composition elemental mapping. It has been shown that through fs pumping the QDs dispersed in toluene show optical gain for appropriate pump power. Also, TA signal has been deconvoluted to extract stimulated emission. It has been seen that the strength of the stimulated emission increases with pump power. By analyzing the TA bleach decay, optical gain lifetime of the QDs has been obtained. The amplification properties of the QDs through CW pumping at room temperature is reported. The amplification shows a nonlinear increase with pump power. Our results demonstrate that the $Cd_{1-x}Zn_xSe/ZnSe$ QDs show light amplification through CW pumping at room temperature. However, the threshold for ASE using these exotic QDs is quite high ($31\ \mathrm{W/cm^2}$). The next target would be to reduce the threshold by engineering the core of the QDs for further reduction in auger recombination and thus improving the feedback

Optical Materials EXPRESS

system. Also, we are trying to develop a better heat sink using polymer for stabilizing the temperature of the system.

Funding. Ministry of Education, India (IE/REDA-23-2109.19); Ministry of Electronics and Information technology (MEITY), India (SP/MITO-19-0005).

Acknowledgments. The author would like to thank MEITY, MHRD for financial assistance and CENSE, IISc for TEM facility. Authors would also like to thank Dr. Suchita for help in experimental setup to observe ASE at RT in QDs.

Disclosures. The authors declare no conflicts of interest.

Data availability. The data underlying the findings in this research are not currently open to the general public, however, they are available from the authors upon reasonable request.

Supplemental document. See Supplement 1 for supporting content.

Reference

1. P. Geiregat, D. Van Thourhout, and Z. Hens, "A bright future for colloidal quantum dot lasers," NPG Asia Mater **11**(1), 41 (2019).
2. M. Saba, S. Minniberger, F. Quochi, J. Roither, M. Marceddu, A. Gocalinska, M.V. Kovalenko, D.V. Talapin, W. Heiss, A. Mura, and G. Bongiovanni, "Exciton–exciton interaction and optical gain in colloidal CdSe/CdS dot/rod nanocrystals," Adv. Mater. **21**(48), 4942–4946 (2009).
3. C. D. Sonnichsen, T. Kipp, X. Tang, and P. Kambhampati, "Efficient optical gain in CdSe/CdS Dots-in-Rods," ACS Photonics **6**(2), 382–388 (2019).
4. F. García-Santamaría, Y. Chen, J. Vela, R.D. Schaller, J.A. Hollingsworth, and V.I. Klimov, "Suppressed auger recombination in "giant" nanocrystals boosts optical gain performance," Nano Lett. **9**(10), 3482–3488 (2009).
5. Y. Liao, G. Xing, N. Mishra, and T. C. Sum, "Yinthai Chan Low threshold, amplified spontaneous emission from core-seeded semiconductor nanotetrapods incorporated into a sol–gel matrix," Adv. Mater. **24**(23), OP159–OP164 (2012).
6. C. She, I. Fedin, D. S. Dolzhnikov, A. Demortière, R. D. Schaller, M. Pelton, and D. V. Talapin, "Low-threshold stimulated emission using colloidal quantum wells," Nano Lett. **14**(5), 2772–2777 (2014).
7. J. Q. Grim, S. Christodoulou, F. Di Stasio, R. Krahne, R. Cingolani, L. Manna, and I. Moreels, "Continuous-wave biexciton lasing at room temperature using solution-processed quantum wells," Nat. Nanotechnol. **9**(11), 891–895 (2014).
8. G. Xing, M. Nripan, S.S. Lim, N. Yantara, X. Liu, D. Sabba, M. Grätzel, S. Mhaisalkar, and T.C. Sum, "Low-temperature solution-processed wavelength-tunable perovskites for lasing," Nat. Mater. **13**(5), 476–480 (2014).
9. S. Yakunin, L. Protesescu, F. Krieg, M.I. Bodnarchuk, G. Nedelcu, M. Humer, G. De Luca, M. Fiebig, W. Heiss, and M.V. Kovalenko, "Low-threshold amplified spontaneous emission and lasing from colloidal nanocrystals of caesium lead halide perovskites," Nat. Commun. **6**(1), 8056 (2015).
10. H. Zhu, Y. Fu, F. Meng, X. Wu, Z. Gong, Q. Ding, M. V. Gustafsson, M. Tuan Trinh, S. Jin, and X-Y. Zhu, "Lead halide perovskite nanowire lasers with low lasing thresholds and high quality factors," Nat. Mater. **14**(6), 636–642 (2015).
11. Y.-S. Park, W. K. Bae, L. A. Padilha, J. M. Pietryga, and V. I. Klimov, "Effect of the core/shell interface on Auger recombination evaluated by single-quantum-dot spectroscopy," Nano Lett. **14**(2), 396–402 (2014).
12. V. I. Klimov, S. A. Ivanov, J. Nanda, M. Achermann, I. Bezel, J. A. McGuire, and A. Piryatinski, "Single-exciton optical gain in semiconductor nanocrystals," Nature **447**(7143), 441–446 (2007).
13. Kaifeng Wu, Young-Shin Park, Jaehoon Lim, and Victor I. Klimov, "Towards zero-threshold optical gain using charged semiconductor quantum dots," Nat. Nanotechnol. **12**(12), 1140–1147 (2017).
14. Cuong Dang, Joonhee Lee, Kwangdong Roh, Hanbit Kim, Sungmo Ahn, Heonsu Jeon, Craig Breen, J. S. Steckel, Seth Coe-Sullivan, and Arto. Nurmikko, "Highly efficient, spatially coherent distributed feedback lasers from dense colloidal quantum dot films," Appl. Phys. Lett. **103**(17), 171104 (2013).
15. K. Roh, C. Dang, J. Lee, S. Chen, J. S. Steckel, S. Coe-Sullivan, and A. Nurmikko, "Surface-emitting red, green, and blue colloidal quantum dot distributed feedback lasers," Opt. Express **22**(15), 18800–18806 (2014).
16. C. Dang, J. Lee, C. Breen, J. S. Steckel, S. Coe-Sullivan, and A. Nurmikko, "Red, green and blue lasing enabled by single-exciton gain in colloidal quantum dot films," Nat. Nanotechnol. **7**(5), 335–339 (2012).
17. B. Ellis, M. A. Mayer, G. Shambat, T. Sarmiento, J. Harris, E. E. Haller, and J. Vuckovic, "Ultralow-threshold electrically pumped quantum-dot photonic-crystal nanocavity laser," Nat. Photonics **5**(5), 297–300 (2011).
18. M. Nomura, N. Kumagai, S. Iwamoto, Y. Ota, and Y. Arakawa, "Photonic crystal nanocavity laser with a single quantum dot gain," Opt. Express **17**(18), 15975–15982 (2009).
19. B. Guzelturk, Y. Kelestemur, M. Olutas, S. Delikanli, and H. V. Demir, "Amplified spontaneous emission and lasing in colloidal nanoplatelets," ACS Nano **8**(7), 6599–6605 (2014).
20. C. She, I. Fedin, D. S. Dolzhnikov, P. D. Dahlberg, G. S. Engel, R. D. Schaller, and D. V. Talapin, "Red, yellow, green, and blue amplified spontaneous emission and lasing using colloidal cdse nanoplatelets," ACS Nano **9**(10), 9475–9485 (2015).

Optical Materials EXPRESS

21. P. Brenner, O. Bar-On, M. Jakoby, I. Allegro, B.S. Richards, U.W. Paetzold, I.A. Howard, J. Scheuer, and U. Lemmer, "Continuous wave amplified spontaneous emission in phase-stable lead halide perovskites," Nat Commun. **10**(1), 988 (2019).
22. P. Geiregat, A.J. Houtepen, L.K. Sagar, I. Infante, F. Zapata, V. Grigel, G. Allan, C. Delerue, D. Van Thourhout, and Z. Hens, "Continuous-wave infrared optical gain and amplified spontaneous emission at ultralow threshold by colloidal HgTe quantum dots," Nat. Mater. **17**(1), 35–42 (2018).
23. D. Yan, T. Shi, Z. Zang, T. Zhou, Z. Liu, Z. Zhang, J. Du, Y. Leng, and X. Tang, "Ultrastable $CsPbBr_3$ perovskite quantum dot and their enhanced amplified spontaneous emission by surface ligand modification," Small **15**, 1901173 (2019).
24. C. Li, C. Han, Y. Zhang, Z. Zang, M. Wang, X. Tang, and J. Du, "Enhanced photoresponse of self-powered perovskite photodetector based on ZnO nanoparticles decorated $CsPbBr_3$ films," Sol. Energy Mater. Sol. Cells **172**, 341–346 (2017).
25. D. Yan, T. Shi, Z. Zang, S. Zhao, J. Du, and Yuxin Leng, "Stable and low-threshold whispering-gallery-mode lasing from modified $CsPbBr_3$ perovskite quantum dots@SiO_2 sphere," Chem. Eng. J. **401**, 126066 (2020).
26. Q. Mo, T. Shi, W. Cai, S. Zhao, D. Yan, J. Du, and Z. Zang, "Room temperature synthesis of stable silica-coated $CsPbBr_3$ quantum dots for amplified spontaneous emission," Photonics Res. **8**(10), 1605–1612 (2020).
27. L. Wang, L. Meng, L. Chen, S. Huang, X. Wu, G. Dai, L. Deng, J. Han, B. Zou, C. Zhang, and H. Zhong, "Ultralow-threshold and color-tunable continuous-wave lasing at room-temperature from in situ fabricated perovskite quantum dots," J. Phys. Chem. Lett. **10**(12), 3248–3253 (2019).
28. L. Jiang, R. Liu, R. Su, Y. Yu, H. Xu, Y. Wei, Z.K. Zhou, and X. Wang, "Continuous wave pumped single-mode nanolasers in inorganic perovskites with robust stability and high quantum yield," Nanoscale **10**(28), 13565–13571 (2018).
29. H. Zhang, C. Zou, Y. Chen, L. Wu, W. Wen, B. Du, S. Feng, J. Shang, C. Cong, and T. Yu, "Continuous-wave vertical cavity surface-emitting lasers based on single crystalline lead halide perovskites," Adv. Opt. Mater. **9**(13), 2001982 (2021).
30. H. Zhang, Y. Hu, W. Wen, B. Du, L. Wu, Y. Chen, S. Feng, C. Zou, J. Shang, H. J. Fan, and T. Yu, "Room-temperature continuous-wave vertical-cavity surface-emitting lasers based on 2D layered organic–inorganic hybrid perovskites," APL Materials **9**(7), 071106 (2021).
31. M. S. Alias, Z. Liu, A. Al-Atawi, T. K. Ng, T. Wu, and B. Ooi, "Continuous-wave optically pumped green perovskite vertical-cavity surface-emitter," Opt. Lett. **42**(18), 3618–3621 (2017).
32. C. Qin, A. Sandanayaka, C. Zhao, T. Matsushima, D. Zhang, T. Fujihara, and C. Adachi, "Stable room-temperature continuous-wave lasing in quasi-2D perovskite films," Nature **585**(7823), 53–57 (2020).
33. X. Fan, Z. Mu, Z. Chen, Y. Zhan, F. Meng, Y. Li, G. Xing, and W.-Y. Wong, "An efficient green-emitting quantum dot with near-unity quantum yield and suppressed Auger recombination for high-performance light-emitting diodes," Chem. Eng. J. **461**, 142027 (2023).
34. J. Cho, Y. K. Jung, J.-K. Lee, and H.-S. Jung, "Highly efficient blue-emitting CdSe-derived core/shell gradient alloy quantum dots with improved photoluminescent quantum yield and enhanced photostability," Langmuir **33**(15), 3711–3719 (2017).
35. Y.-S. Park, W. K. Bae, T. Baker, J. Lim, and V. I. Klimov, "Effect of Auger Recombination on Lasing in Heterostructured Quantum Dots with Engineered Core/Shell Interfaces," Nano Lett. **15**(11), 7319–7328 (2015).
36. W. K. Bae, L. A. Padilha, Y.-S. Park, H. McDaniel, I. Robel, J. M. Pietryga, and V. I. Klimov, "Controlled Alloying of the Core–Shell Interface in CdSe/CdS Quantum Dots for Suppression of Auger Recombination," ACS Nano **7**(4), 3411–3419 (2013).
37. L. K. Sagar, G. M. Bappi, A. Johnston, B. Chen, P. Todorović, L. Levina, M. I. Saidaminov, F. P. G. de Arquer, D.-H. Nam, M.-J. Choi, S. Hoogland, O. Voznyy, and E. H. Sargent, "Suppression of Auger Recombination by Gradient Alloying in InAs/CdSe/CdS QDs," Chem. Mater. **32**(18), 7703–7709 (2020).
38. X. Wang, X. Ren, K. Kahen, M A. Hahn, M. Rajeswaran, S. Maccagnano-Zacher, J. Silcox, G. E. Cragg, A. L. Efros, and T. D. Krauss, "Non-blinking semiconductor nanocrystals," Nature **459**(7247), 686 (2009).
39. D. Ahn, T.-K. Yoo, and H. Y. Lee, "Optical gain of CdZnSe/ZnSe quantum well lasers," Appl. Phys. Lett. **59**(21), 2669–2671 (1991).
40. M. A. Haase, J. Qiu, J. M. DePuydt, and H. Cheng, "Blue-green laser diodes," Appl. Phys. Lett. **59**(11), 1272–1274 (1991).
41. Q. Zhang, C. Nie, C. Chang, C. Guo, X. Jin, Y. Qin, F. Li, and Q. Li, "Highly luminescent red emitting CdZnSe/ZnSe quantum dots synthesis and application for quantum dot light emitting diodes," Opt. Mater. Express **7**(11), 3875–3884 (2017).
42. Y. V. Vandyshev, V. S. Dneprovskii, V. I. Klimov, and D. K. Okorokov, "Lasing on a transition between quantum-well levels in a quantum," Jetp Lett **54**(8), 442 (1991).
43. X. Huang, X. Feng, L. Chen, L. Wang, W. C. Tan, L. Huang, and K.-W. Ang, "Fabry-Perot cavity enhanced light-matter interactions in two-dimensional van der Waals heterostructure," Nano Energy **62**, 667–673 (2019).